Computer Assisted Methods in Engineering and Science, **20**: 99–112, 2013.

TWENTY YEARS OF THE CAMES

Optimization of functionally gradient materials in valve design under cyclic thermal and mechanical loading

Grzegorz Maciejewski, Zenon Mróz
Institute of Fundamental Technological Research, Polish Academy of Sciences
Pawińskiego 5B, 02-106 Warsaw, Poland
e-mail: gmaciej@ippt.pan.pl

The robust and simple optimization method of functionally graded material (FGM) for combined cyclic thermal and mechanical loading with application to valve design is proposed.

The optimization procedure starts from the homogeneous ceramic material distribution and after thermomechanical analysis of the whole process, the new distribution of material is determined by reducing concentration of the ceramic phase at places of high tensile stresses and by increasing ceramic contents at places of high effective stresses. The optimal distribution of ceramic phase is found through iterations. We have shown the numerical example of the proposed method for optimization of a composite exhaust valve of combustion engine. The example illustrates the optimal density distribution of ceramic phase of Al_2O_3 within NiAl matrix. In the design study we have used the transient analysis of stress and temperature fields.

The proposed method shares merits of standard optimization and topology optimization, it allows for creating one phase of material inside the other. It can be especially useful to problems of structural elements subjected to thermomechanical loading histories.

Keywords: thermomechanical analysis, high frequency cyclic loading, coating, design, FGM, optimization.

1. Introduction

Thermal stresses play crucial role in many areas of engineering. In some engineering structures like car engines, turbine blades, aerospace structures, energy conversion systems, which work at high and non-uniform temperature fields, designing of the thermal resistant structures is of primary importance.

Thermal stresses in transient state can be excessively large and generate cracks. Such a situation occurs in engine exhaust valves which control gas efflux from internal combustion engines. Currently used valves are the result of many years of development, tests and checks. Exploitation of standard valves made of a uniform material under high and inhomogeneous temperature field results in numerous cases of excessive plastic deformations inducing valve geometry changes, gas leakage, and formation of cracks leading to eventual failure. Additionally, highly corrosive environment and mechanical contact between engine parts may lead to excessive wear. Conventional steel valves have relatively high specific weight and operate at relatively high contact friction thus leading to higher dissipation and higher CO_2 emission during operation. When alternative fuels were used, like, e.g., compressed natural gas, the increased wear effect has been observed. The necessity to reduce energy consumption and need for a longer service lifetime of mechanical parts implies application of new advanced materials.

Recently, the interest of production of low-weight, thermal resistant valves in combustion engines has been strongly intensified due to economical and ecological aspects of car engine operation. Ce-

ramic materials, thanks to their excellent properties at high temperatures, low specific weight, and good wear resistance are currently viewed as promising materials for thermal coatings. It seems that they could be applied to production of engine exhaust valve. However, thermal properties of ceramic coatings usually differ from those of the corresponding bulk materials. Especially, the difference of thermal expansion coefficient between ceramic coating and bulk material leads, in the case of temperature loading, to high thermal stresses at their interfaces. To minimize stress concentration at the interfaces, the multi-phase material with smooth transition between phases can be designed and produced. This is a concept of functionally graded material (FGM). FGM is a composite material with the volume fractions of the constituents varying gradually in the designed profile. It is usually a mixture of ceramic and metal phases. The ceramic phase provides high temperature resistance because of its low thermal conductivity, while a ductile metal phase prevents fracture caused by the stress concentrations in the inhomogeneous structure. The design of composition distribution within FGM for a particular need is a challenging task.

The composition distribution within FGM can be designed in a systematic way by the optimization procedure [20]. The optimization method is strictly related to the area of applicability of FGM. The objective function of optimization depends on the problem considered and usually includes a measure of stress level [3, 6], fracture resistance, temperature distribution [14, 20], strain energy density and peaks of effective stresses. As design parameters one can select for instance thickness and volume fraction of FGM interlayers or their shapes and micromechanical layout of inclusions. The review of optimization procedures of FGM can be found in [2]. A separate class of optimization approaches constitutes the topology optimization [1, 10]. The topology optimization can be viewed as a process of generation and changing position or shape of material interfaces in pseudo-time. The material interfaces are treated as the zero level set functions [15, 17]. The evolution of these functions will result in varying shape of material interfaces. However, the implementation of this procedure may be problematic. In fact, the optimality criterion may imply creation of one phase inside the other phase. To allow this, the material topological derivative should be applied. Examples of topological optimization can be found in [4, 16, 21].

To obtain an FGM structure which is resistant to thermomechanical loading, minimizing thermal stresses are of primary importance. In the case of engine valves with surface coatings, thermal stresses at interfaces are very high [19]. Joining two or more materials together is usually accompanied by generation of interface stresses. The valve with standard FGM coating does not provide long-term service under such conditions. To solve the problem of joining two materials being under combined cyclic thermal and mechanical loadings, we propose the robust optimization method of FGM. As a theoretical background for finding the optimal distribution of materials in FGM we have selected the multi-criterion optimization methodology. We present design of an exhaust valve of combustion engine, see Fig. 1 and the schematic representation of the axisymmetric valve model in Fig. 2. The problem is reduced to specify distribution of smooth evolution of material phases. The design of the structure subjected to high cyclic thermal loading becomes possible by replacing this loading by its simplified representation. The metal-matrix composite valve is optimized to gain

Fig. 1. An example of light valve of a graded metal matrix composite under investigation (courtesy of Institute of Materials Research of Slovak Academy of Sciences, Bratislava).

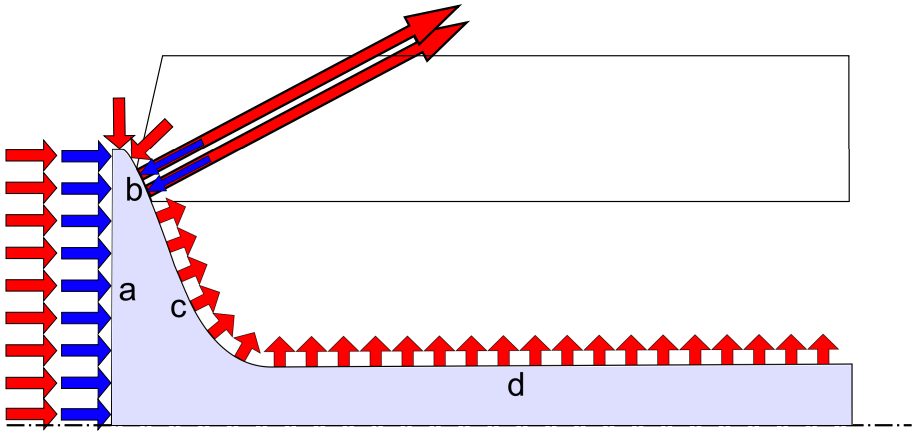

Fig. 2. The axisymmetric valve model used in the finite element simulations. The valve is subjected to mechanical loading at interfaces a (pressure) and b (contact with the engine), while thermal fluxes act at interfaces a, b, c, and d (marked with red colour). Assumed valve dimensions: a half of head diameter (along the face a) is equal 12 mm; horizontal length (along symmetry axis) is equal 35 mm.

its resistivity against cracking and assuring safety with respect to excessive plastic flow. The wear resistance control at contact interfaces is not considered in this paper.

2. Thermomechanical stress analysis

We consider a thermo-elastic body without body forces and in the absence of internal heat sources. For small strain formulation adopted here the balance and constitutive equations take the following form:

$$\sigma_{ij,j} = 0, \tag{1}$$

$$\sigma_{ij} = C_{ijkl}\,\epsilon_{kl} - \beta_{ij}(T - T_0), \tag{2}$$

and

$$q_{i,i} = \rho\, c \dot{T}, \tag{3}$$

$$q_i = -\lambda T_{,i}, \tag{4}$$

where σ denotes the Cauchy stress tensor, ϵ is the total strain tensor, $\mathbf{q}$ is the heat flux vector, ρ, c, T, T_0, λ are mass density, specific heat, instantaneous absolute valve temperature, environmental reference temperature, thermal conductivity coefficient respectively, and $\mathbf{C}$ is the elastic stiffness tensor. The summation convention for repeated indices is used. For isotropic materials with the thermal expansion coefficient α, the elastic modulus E, and the Poisson ratio ν, the thermoelastic tensor is defined as $\beta_{ij} = \delta_{ij}\,\beta = \delta_{ij}\,\alpha E/(1-\nu)$. Additionally to Eq. (4), the heat flux between surface of the body and surroundings is described by the formula

$$q = -h_c\,(T_s - T_v), \tag{5}$$

in which h_c, T_s, and T_v denote the thermal contact conductance coefficient, temperature of the surrounded medium and temperature of the body external surface. Generally, the value of the contact conductance coefficient depends on surface state (roughness, oxide layer, pore concentration in subsurface layer, etc.) and on pressure and shear stress acting on the surface. The vector of heat transfer at the body surface is oriented perpendicularly to the surface. The boundary and initial conditions assumed here are as follows:

$$\sigma_{ij}\,n_j = f_i \qquad \text{on} \quad \partial\Omega_f \times (t_0, t_{fin}), \tag{6}$$

$$u_i = \overline{u}_i \qquad \text{on} \quad \partial\Omega_u \times (t_0, t_{fin}), \tag{7}$$

while contact conditions are specified by the Signorini complementarity conditions

$$\left.\begin{aligned} p_n \geq 0, \quad d_n \geq 0 \\ p_n\, d_n = 0 \end{aligned}\right\} \qquad \text{on} \quad \partial\Omega_c \times (t_0, t_{fin}), \tag{8}$$

where n_j is the outward normal unit vector to the boundary $\partial\Omega$ of the body occupying volume Ω, f_i is the prescribed surface force, $\overline{u}_i$ is the prescribed displacement vector, p_n is the contact pressure, d_n is the standard gap variable, t_0 and t_{fin} are initial and final instants of time. When contact occurs, the contact pressure is positive and the gap vanishes, while during separation $p_n = 0$ and $d_n > 0$. Additionally, we have $\partial\Omega = \bigcup(\partial\Omega_f + \partial\Omega_u + \partial\Omega_c)$ and $\bigcap(\partial\Omega_f + \partial\Omega_u + \partial\Omega_c) = \emptyset$. The thermal boundary and initial conditions

$$T = \overline{T} \qquad \text{on} \quad \partial\Omega_T \times (t_0, t_{fin}), \tag{9}$$

$$q_i\, n_i = \overline{q} \qquad \text{on} \quad \partial\Omega_q \times (t_0, t_{fin}), \tag{10}$$

$$T_s = \overline{T}_s \qquad \text{on} \quad \partial\Omega_s \times (t_0, t_{fin}), \tag{11}$$

$$T_0 = \overline{T}_0 \qquad \text{in} \quad \Omega \times t_0, \tag{12}$$

are enforced through prescribed temperature $\overline{T}$, prescribed heat flux $\overline{q}$, prescribed ambient temperature $\overline{T}_s$, initial temperature $\overline{T}_0$, and complementary conditions: $\partial\Omega = \bigcup(\partial\Omega_T + \partial\Omega_q + \partial\Omega_s)$, $\bigcap(\partial\Omega_T + \partial\Omega_q + \partial\Omega_s) = \emptyset$.

The effective physical properties of heterogenous material depend on particular microstructure and volume fraction of components. From many methods of averaging, the mean value of the Hashin-Shtrikman bounds [11] for bulk (denoted by K) and shear (denoted by G) moduli of the material with the specific phase composition x of ceramic phase (subscript c) within metal matrix (subscript m) are explored:

$$K = (1-x)K_m + xK_c - \frac{1}{2}\left(\frac{(1-x)x(K_c - K_m)^2}{(1-x)K_c + xK_m + G_c} + \frac{(1-x)x(K_c - K_m)^2}{(1-x)K_c + xK_m + G_m}\right), \tag{13}$$

$$G = (1-x)G_m + xG_c - \frac{1}{2}\left(\frac{(1-x)x(G_c - G_m)^2}{(1-x)G_c + xG_m + \dfrac{K_c G_c}{K_c + 2\,G_c}} + \frac{(1-x)x(G_c - G_m)^2}{(1-x)G_c + xG_m + \dfrac{K_m G_m}{K_m + 2\,G_m}}\right), \tag{14}$$

for elastic stiffness coefficients (the randomly positioned particles are assumed). For all other material parameters (denoted as P) like yield strength, thermal conductivity, thermal capacity, and thermal expansion coefficient, the simple Vegard rule was used that is

$$P_i = (1-x)P_m + x\,P_c\,, \qquad x \in \langle 0, 1\rangle, \tag{15}$$

where P_m and P_c denote particular material properties of metal and ceramic phase respectively. Usually, the thermal and mechanical parameters are temperature dependent. But the temperature dependence of the yield and crack resistivity for the analysed metal-matrix composite is not available. The cyclic loading additionally complicates mechanical characterization. Therefore, such a dependence is not considered here and the fixed values were taken for numerical analysis. Some remarks are necessary on the tensile strength of composite material. Under monotonic loading, the tensile strength of a composite with low ceramic content generally increases. But under cyclic loading the mechanical behaviour of particle reinforced composites may be different. Mechanical

properties of particle reinforced composites depend on size, shape, and spacing of precipitates [5]. Additionally, at high temperatures, the difference between thermal expansion coefficients of metal matrix and ceramic phase leads to a high concentration of stresses at inclusion interfaces. These concentrations (depending on shape of inclusions), under high-cycle loading, generally lead to decrease of the tensile strength of composite. Therefore, for safe design, the monotonic decrease of the tensile strength versus ceramic content is assumed. The crack resistivity σ_{cr}^{lim} and yield resistivity σ_{ef}^{lim} depend on the specific phase composition at each point through relation (15).

3. Thermomechanical analysis – simplifying assumptions

Let us consider an engine exhaust valve schematically illustrated in Fig. 2. The valve is subjected to mechanical loading, marked by blue colour, and to thermal transient loading, marked by red colour. The numerical analysis of valve, see, for example [19], shows that, at the interface between ceramic coating and the metal substrate, very high stresses are observed. Additionally, when the valve is subjected to cyclic thermal loading, as presented in [18], the numerical optimization becomes very complex. Without simplification of the model, the optimization would not be feasible, requiring excessive computer time. Therefore, the simplification of boundary conditions is proposed in order to account for physical aspects of analysed process and to allow for optimization procedure.

3.1. Simplified analysis of high-cycle thermal and mechanical loading

The simplification of boundary conditions is performed by replacing the true thermal loading by its averaged values over one cycle of engine operation, while the mechanical loading condition corresponds to maximum value of loading during one cycle. Thus, our simplification is based on replacement of the high cyclic thermal and mechanical load variations by the *equivalent steady heat flow* conditions in each cycle and *the most unfavourable static loading*. Simplification of the thermal load seems to be rational because the engine operation cycle periods are small as compared to time period for specified temperature variation. The mechanical load can be separated into nonzero pressure load on the valve head applied during combustion process (for the valve closed and the contact interaction at the valve seat) and zero pressure during remaining time period (and vanishing load at contact interface for the valve open). For mechanical analysis we take only the external load, without averaging over the engine cycle. The above simplifications allow us to replace the complex dynamic interaction by the equivalent, steady states for each cycle. These simplifications also allow for an effective optimization within a reasonable time.

The heat transfer between the valve and surroundings is described by Eq. (5). Table 1 presents values of the contact conductance coefficient and ambient temperatures around the valve. The values of the contact conductance coefficient h_c and ambient temperature are based on data from [18, 22] and from unpublished sources (FIAT data). The gas pressure is assumed to be equal to 60 kPa. The mechanical parameters of metal (subscript m) and ceramic phase (subscript c) are as follows: $\rho_m = 8200$, $\rho_c = 3880$ (the mass density [kg/m^3]); $c_m = 1030$, $c_c = 880$ (the specific heat [J/(kg K)]);

Table 1. Contact conductance coefficients and ambient temperatures around the valve, see detailed description in Fig. 2.

contact zone between the valve and	h_c [W/m^2 °C]	T_s [°C]
gases in cylinder	850	900
valve seat	3000	500
exhaust port	500	500
valve guide	2000	400

$\lambda_m = 20.0$, $\lambda_c = 26.5$ (the conductivity coefficient [W/(m K)]); $\alpha_m = 15.0 \cdot 10^{-6}$, $\alpha_c = 8.1 \cdot 10^{-6}$ (the thermal expansion coefficient [1/K]); $E_m = 223$, $E_c = 330$ (the elastic modulus [GPa]); $\nu_m = 0.30$, $\nu_c = 0.22$ (the Poisson ratio); $\sigma_{ef\,m}^{lim} = 0.74$, $\sigma_{ef\,c}^{lim} = 0.85$ (the yield resistivity [GPa]); $\sigma_{cr\,m}^{lim} = 1.30$, $\sigma_{cr\,c}^{lim} = 0.10$ (the crack resistivity [GPa]).

The particular numerical implementation of axisymmetric valve model in examples shown in the next sections is as follows: eight-node serendipity element [12], the area is divided into around 3000 elements, the length of time step can be equal or larger than the engine operation cycle and is set as $\triangle t = 1\,s$, the transient problem is integrated with the backward Euler method and the actual volume fraction distribution of ceramic phase is updated at each Gauss point. The implemented procedures with small modifications can also be applied to the finite strain formulation.

4. The proposed optimization method

The proposed methodology explores two parameters as a measure of tensile stress and effective plastic stress during process of transient thermal loading. The first is the maximum tensile stress $\sigma_{cr} = \sigma_1 > \sigma_2 > \sigma_3$ at a particular point and at a particular time instant and the second is the effective von Mises stress $\sigma_{ef} = (3/2\,\mathbf{s} \cdot \mathbf{s})^{1/2}$, where $\mathbf{s}$ is the stress deviator. Performing simulation of the whole process, we can extract maximum values of σ_{cr} and σ_{ef} during the process. As the scaling parameters, the crack resistivity σ_{cr}^{lim} and yield resistivity σ_{ef}^{lim} at each point are taken.

The optimization procedure starts from the uniform distribution of ceramic phase. We want to reduce concentration of the ceramic phase at places of high tensile stresses and increase the ceramic phase density at places of high effective stresses. A balance between those two objectives leads to an optimal design in the sense of the multicriterion objective functional providing the optimal distribution of ceramic phase. The optimization problem of FGM profile is formulated as follows: specify the field of distribution of ceramic phase volume fraction x within the metal matrix, such that the effects of maximum tensile and effective stresses are balanced. This balance is controlled through the weight factor β.

The time and volume objective functional in the global form for the transient process combining cracking and plastic deformation constraints can be proposed as follows:

$$J_{obj} = \int_{t_0}^{t_{fin}} \int_V \left[\left(\frac{\sigma_{ef}}{\sigma_{ef}^{lim}} \right)^m + \beta \left(\frac{\sigma_{cr}}{\sigma_{cr}^{lim}} \right)^m \right] d\Omega\, dt, \tag{16}$$

where $m \geq 1$ is the localization control parameter. The m factor in Eq. (16) specifies the degree of assessment of stress local values. For low values of m (typically $m = 1 \div 5$) the local peak values are averaged by volume integration. However, for larger values of m, the local stress concentration peaks are exhibited and they significantly affect the value of the objective functional. On the other hand, the local objective function is proposed in the form:

$$J_{obj} = \left[\frac{\sigma_{ef}}{\sigma_{ef}^{lim}} + \beta \frac{\sigma_{cr}}{\sigma_{cr}^{lim}} \right] \tag{17}$$

and its distribution in element domain can be specified and used in redesign procedure. Here the crack resistivity σ_{cr}^{lim} and the yield resistivity σ_{ef}^{lim} depend on their initial values $\sigma_{cr\,0}^{lim}$, $\sigma_{ef\,0}^{lim}$ and on the specific phase composition x:

$$\sigma_{ef}^{lim} = \sigma_{ef\,0}^{lim} (1 + A\,x), \tag{18}$$

$$\sigma_{cr}^{lim} = \sigma_{cr\,0}^{lim} (1 - B\,x), \tag{19}$$

where A and B are material parameters. The variation of the objective functional (17) with respect to volumetric ceramic phase fraction x takes the form

$$\delta J_{obj} = -\left(\frac{\sigma_{ef}}{\sigma_{ef}^{lim\,2}}\,\delta\sigma_{ef}^{lim} + \beta\frac{\sigma_{cr}}{\sigma_{cr}^{lim\,2}}\,\delta\sigma_{cr}^{lim}\right) + \left(\frac{1}{\sigma_{ef}^{lim}}\,\delta\sigma_{ef} + \beta\frac{1}{\sigma_{cr}^{lim}}\,\delta\sigma_{cr}\right), \tag{20}$$

where the first bracketed term presents the explicit variations of limit stress values due to variation of the ceramic phase concentration factor x and the second term contains implicit variations (or derivatives) of the effective and maximum tensile stress values. The sensitivity variation of σ_{ef} and σ_{cr} can be specified by applying the direct or adjoint structure approaches of sensitivity analysis. The general methodology and description of direct and adjoint methods for the thermo-elastic stress analysis have been presented in [7–9, 13].

Consider here the specification of sensitivity stress variations by the direct method. It is assumed that boundary constraints are fixed. Only the volume fraction parameter x varies. In view of Eq. (2) we can write

$$\delta\sigma_{ij} = C_{ijkl}\,\delta\epsilon_{kl} + \delta C_{ijkl}\,\epsilon_{kl} - \beta_{ij}\delta T - \delta\beta_{ij}(T - T_0). \tag{21}$$

The stress variation field satisfies the equilibrium equation

$$\delta\sigma_{ij,j} = 0, \tag{22}$$

and boundary conditions

$$\delta\sigma_{ij}\,n_j = 0 \qquad \text{on} \quad \partial\Omega_f, \tag{23}$$

$$\delta u_i = 0 \qquad \text{on} \quad \partial\Omega_u. \tag{24}$$

So, we have

$$\left[C_{ijkl}\,\delta\epsilon_{kl} - \beta_{ij}\delta T\right]_{,j} = \left[\delta\beta_{ij}(T - T_0) - \delta C_{ijkl}\,\epsilon_{kl}\right]_{,j}. \tag{25}$$

The thermal sensitivity field with respect to varying volumetric factor x can be specified from the heat conduction and balance equations, see Eqs. (3) and (4):

$$\lambda\delta T_{,ii} + \lambda_i\delta T_{,i} - \rho\delta\dot{T} = \delta\lambda T_{,ii} + \delta\lambda_{,i}T_{,i} \tag{26}$$

and the boundary conditions

$$\delta q_i n_i = 0 \qquad \text{on} \quad \partial\Omega_q, \tag{27}$$

$$\delta T = 0 \qquad \text{on} \quad \partial\Omega_T. \tag{28}$$

The coupled system of equations (25) and (26) with boundary conditions (23), (24) and (27), (28) provides the implicit variations $\delta\sigma$ and δT which next can be used in determining variation δJ_{obj} according to Eq. (20). This variation can now be expressed as follows:

$$\delta J_{obj} = -\left(J_{pl} - \beta J_{cr}\right)\,\delta x + \left(K_{ef} - \beta K_t\right)\,\delta x = \left[-\left(J_{pl} - K_{ef}\right) + \beta\left(J_{cr} - K_t\right)\right]\,\delta x, \tag{29}$$

where J_{pl} and J_{cr} are non-dimensional measures of tensile and effective stresses relative to their critical values, namely

$$J_{pl} = A\frac{\sigma_{ef}\,\sigma_{ef\,0}^{lim}}{\sigma_{ef}^{lim\,2}}, \tag{30}$$

$$J_{cr} = B\frac{\sigma_{cr}\,\sigma_{cr\,0}^{lim}}{\sigma_{cr}^{lim\,2}}, \tag{31}$$

while

$$K_{ef} = \frac{\partial \sigma_{ef}}{\partial x}, \tag{32}$$

$$K_t = \frac{\partial \sigma_{cr}}{\partial x} \tag{33}$$

are the implicit sensitivity derivatives specified by Eqs. (25) and (26).

The direct sensitivity method can be applied at least in two ways. First, starting iterative redesign procedure and specifying the redesign field $\triangle x$, the induced stress and temperature variations can be specified by solving the set of differential equations (25) and (26). This step is based on the explicit sensitivity derivatives which will be discussed later. The implicit sensitivity derivatives K_{ef} and K_t can then be specified at each redesign point. In the next step of redesign process, the full sensitivity derivative (20) can be applied to generate the subsequent redesign field $\triangle x$. In the alternative approach, the direct sensitivity analysis can be applied by assuming consecutively variations δx at each single redesign point and collecting stress and temperature variations at all other redesign points, thus $\delta T_{(l)} = K^T_{(lm)} \delta x_m$, $\delta \sigma_{ij(lm)} = K^{\sigma}_{ij(lm)} \delta x_m$, where l denotes the position of the sampling point and m is the position of variation of x at the redesign point. This procedure allows for determination of the sensitivity derivatives K_{ef} and K_t. In this paper, we will illustrate the procedure of redesign based on the explicit terms of sensitivity coupled with the state analysis of the optimal solution, thus

$$\delta J_{obj} = -\left(\frac{\sigma_{ef}\, \sigma^{lim}_{ef\,0}}{\sigma^{lim\,2}_{ef}} A - \beta \frac{\sigma_{cr}\, \sigma^{lim}_{cr\,0}}{\sigma^{lim\,2}_{cr}} B \right) \delta x = -\left(J_{pl} - \beta J_{cr} \right) \delta x. \tag{34}$$

The optimality condition is fulfilled when $\delta J_{obj} = 0$ that is when $J_{pl} = \beta J_{cr}$. The complete formulation containing both explicit and implicit sensitivity terms will be discussed in the separate paper by following the sensitivity analysis presented in [7–9, 13]. The optimization method is based on the redesign procedure driven by the explicit sensitivity derivatives. We will describe it in detail in the next section. It is not guaranteed that the global optimum is reached. The proof of uniqueness of optimal design is probably impossible, due to nonlinearity of the analysed processes and properties of materials. However, the proposed method allows for speeding up redesign procedure for highly complex physical processes. Therefore, it may be viewed as a practical redesign method.

5. Optimization procedure

The optimization procedure starts from the uniform ceramic distribution of Al_2O_3 within the metal matrix of NiAl. We have performed optimizations with assumed minimum volume fraction (0%) or with maximum volume fraction (30%) at the beginning of optimization. The iterative design is performed through the following procedure:

1. Initial state – uniform ceramic phase distribution.

2. Perform simulation of thermal transient process (for time period $t_0 - t_{fin}$).
   For each point of the body determines the maximum effective stress ratio σ_{ef} and maximum tensile stress ratio σ_{cr} during the transient process.

$$r^{\max}_{ef} = \max_t \left(\frac{\sigma_{ef}}{\sigma^{lim}_{ef}} \right), \tag{35}$$

$$r^{\max}_{cr} = \max_t \left(\frac{\sigma_{cr}}{\sigma^{lim}_{cr}} \right). \tag{36}$$

Here σ_{ef}^{lim} and σ_{cr}^{lim} are the limit stress values at a particular point at the time instant when the maximum effective and the maximum tensile stresses have been attained, respectively. It is important to notice that maximum values of stress ratios defined by Eqs. (35) and (36) may occur at different time steps of the transient process but their values are introduced into the objective function (17). Such procedure allows for redesign of the ceramic phase content against the most unfavourable stress state along the complete transient process.

3. Then, from Eqs. (30) and (31) calculate derivative of the objective functional (34), with replaced values of stresses by theirs maximum values during the process, see Eqs. (35,36). The ratios $r_{ef}^{\max}$ and $r_{cr}^{\max}$ should be less than one in order to assure that the structure does not change its geometry and quality as an effect of excessive plastic flow or generation of cracks.

4. Redesign of the ceramic content proceeds at each point according to the following equation:

$$\frac{\Delta x}{x_{\max}} = -\omega\,\delta J_{obj} = \omega\,(J_{pl} - \beta J_{cr}), \tag{37}$$

where ω is the proportionality parameter depending on particular problem considered and limit value of ceramic phase density $x_{\max}$, respectively. Additionally, an obvious constraint $0 \leq x \leq x_{\max}$ should be fulfilled.

5. Repeat steps (2)–(4) until some global condition is fulfilled, e.g., $|\delta J_{obj}| < 0.05$ or $\delta J_{obj} > 0$.

By applying the above iteration procedure, an optimal distribution of ceramic phase can be found. Because stress distribution is continuous, the obtained FGM has also continuous distribution of ceramic phase. Thus, the proposed method shares merits of standard shape optimization and topology optimization because it allows for creation of one phase of material inside another. The following numerical example shows practical usefulness of the method.

6. Example of an engine valve optimization

6.1. The optimization of ceramic phase distribution

The heat generated in the valve is transferred to the remaining portion of an engine through the contact surface b and to the air through surfaces c and d, see Fig. 2. Initially the valve is cold and when the engine starts, a very high heat flux from the combustion engine acts on the valve. The temperature of the valve head rapidly increases, while the rest of the valve is still cold. The main source of stress results from the non-uniform temperature distribution and its maximum occurs at the initial instant of engine work. This temperature distribution inhomogeneity leads to high thermal stresses and can induce cracking and plastic flow. As shown in Fig. 4 the parameters J_{cr} and J_{pl} reach highest values at the beginning of engine operation period. In order to avoid cracking and to minimize plastic deformation, the optimization of ceramic phase distribution is performed with procedure proposed in the previous section. For the considered valve case, the weight parameter β was assumed as $\beta = 1.0$, see Eq. (17). The value of parameter ω in Eq. (37) depends on the iterative process and needs to be adjusted through trials and tests. If ω is too high some spurious modes can occur. Because the solution of the proposed algorithm depends on the step length, the parameter ω should be as low as possible. The terminal condition of optimization process is not applied in order to see a wide range of system evolutions.

Figure 3 shows simulation results for a process with the homogeneous distribution of ceramic phase. The maximum values of crack and yield strength parameters are observed at the time $t = 2$ s of the process, see for example, Fig. 3a and Fig. 3b respectively. The optimization iterations are visualized in Fig. 5, where the evolutions of J_{cr} and J_{pl} during transient thermal loading processes with different ceramic phase distributions are shown. After 40 iterations, the final distribution of Al_2O_3 is attained as presented in Fig. 7. Additional iterations after 40 steps of optimization did not

change the ceramic phase distribution. Thus, one can observe that the final stage of optimization could be attained through stopping condition like for instance $\delta J_{obj} < \delta J_{obj}^{crit}$, where δJ_{obj}^{crit} is a selected critical value.

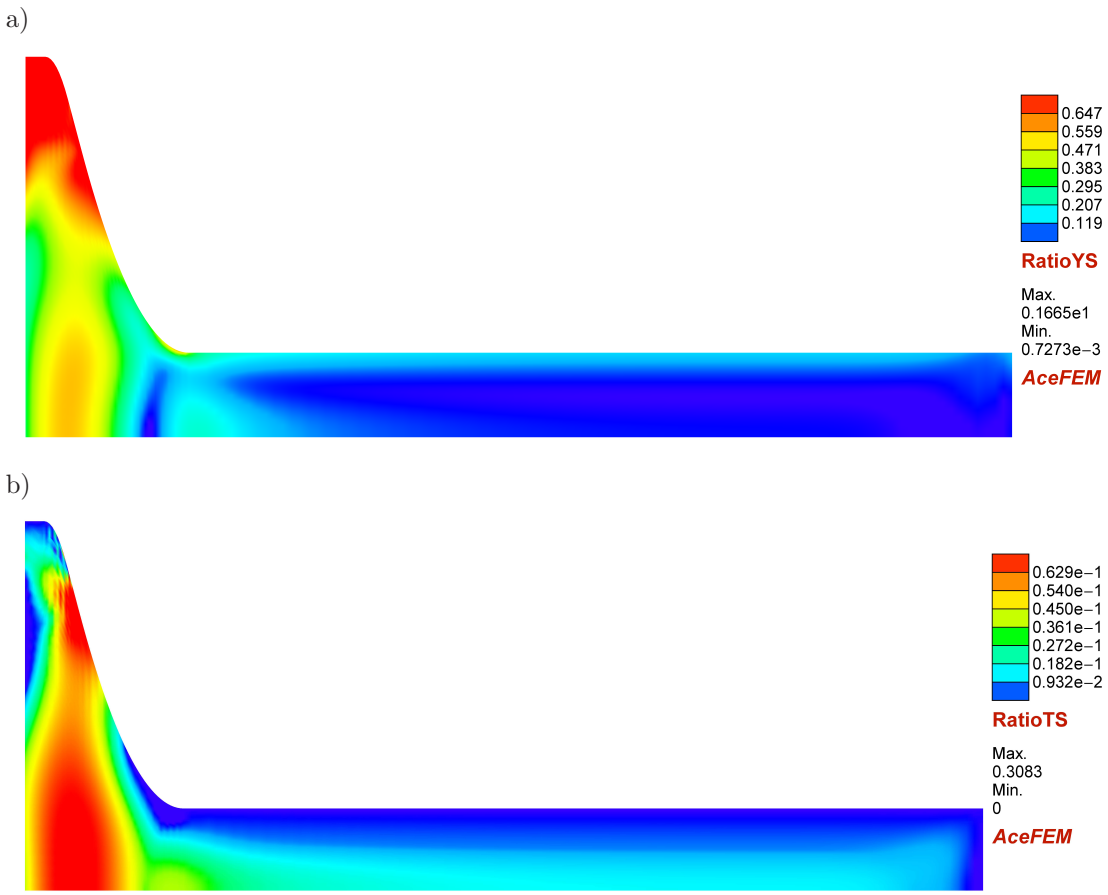

Fig. 3. Analysis of ceramic exhaust valve with initial, homogeneous distribution of ceramic phase Al_2O_3 within NiAl matrix ($x_{ini} = 0.0$); a) and b) distribution of yield strength and crack strength parameters J_{pl} and J_{cr}, defined by Eqs. (30) and (31) respectively at time $t = 2$ s of the process.

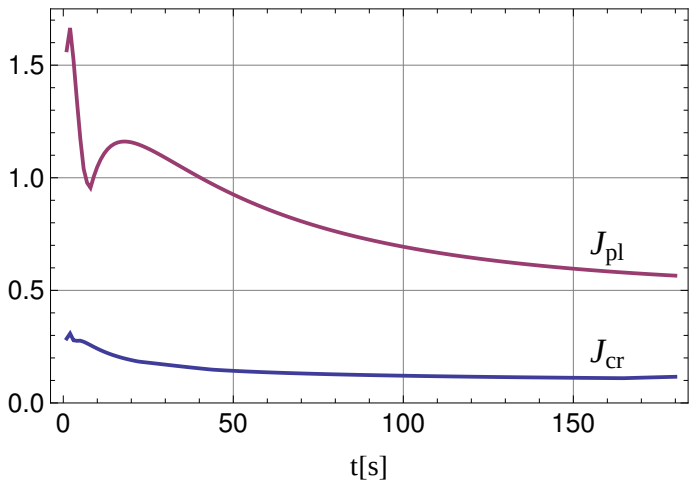

Fig. 4. Time evolution of yield strength and crack strength parameters J_{pl} and J_{cr}, defined by Eqs. (30) and (31) respectively, for uniform metal valve. This is the first iteration from a set of all iterations plotted in Fig. 5.

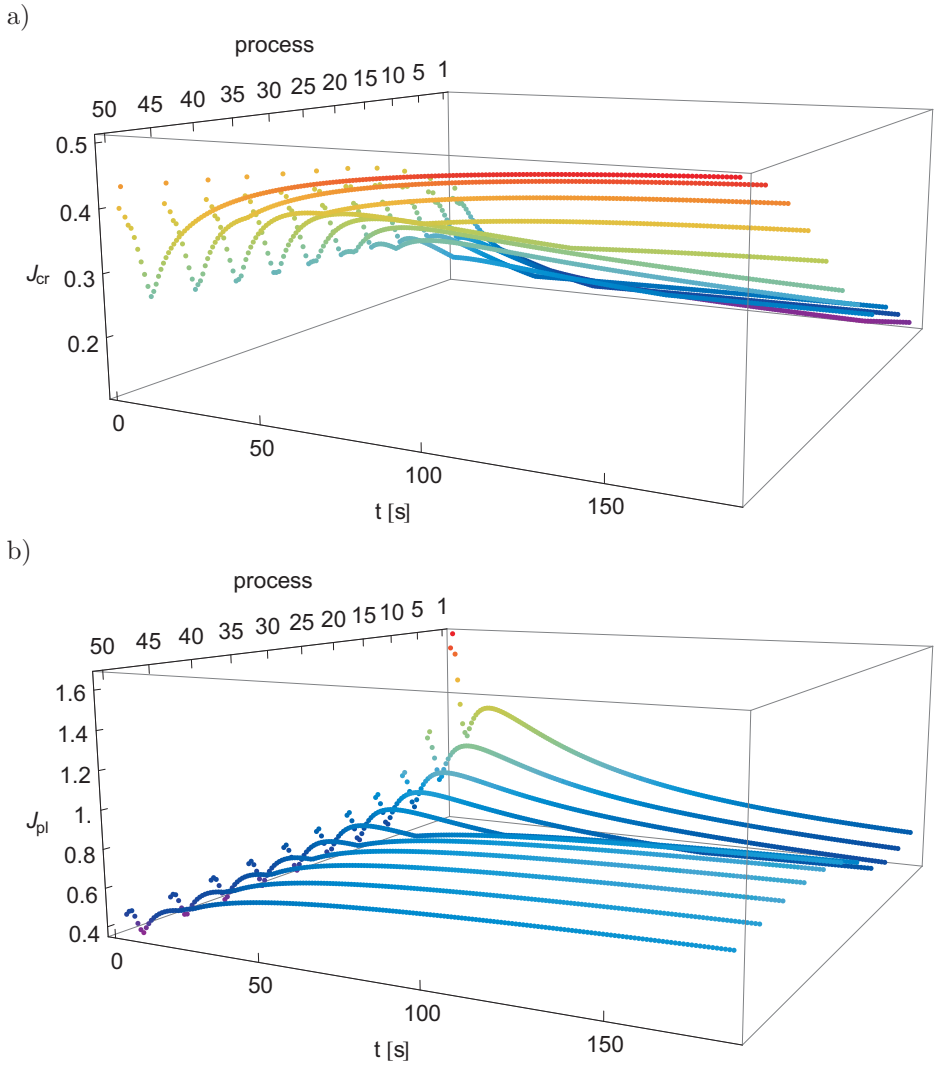

Fig. 5. Iterative process of rebuilding ceramic volume fraction; a) and b) show the evolution of crack strength parameter J_{cr} and yield strength parameter J_{pl} respectively. Thermomechanical loading (combustion process) starts at $t = 0$. There are 50 transient thermomechanical processes, each one for different ceramic phase distribution.

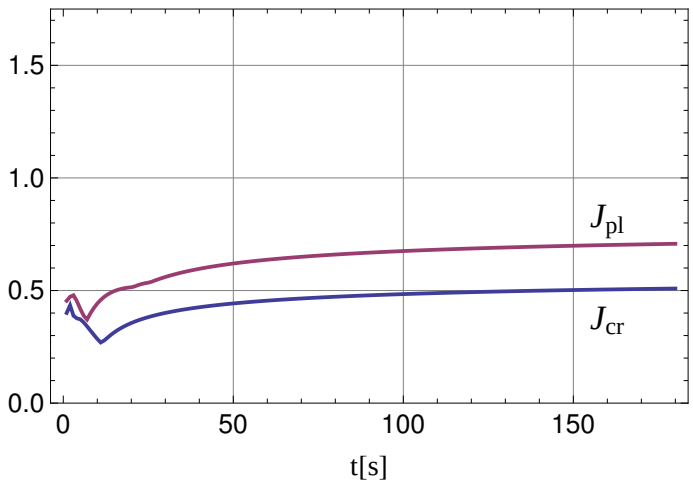

Fig. 6. Time evolution of yield strength and crack strength parameters J_{pl} and J_{cr} for nonuniform metal-ceramic valve with optimized spatial distribution of ceramic phase. This is the last iteration from a set of all iterations plotted in Fig. 5.

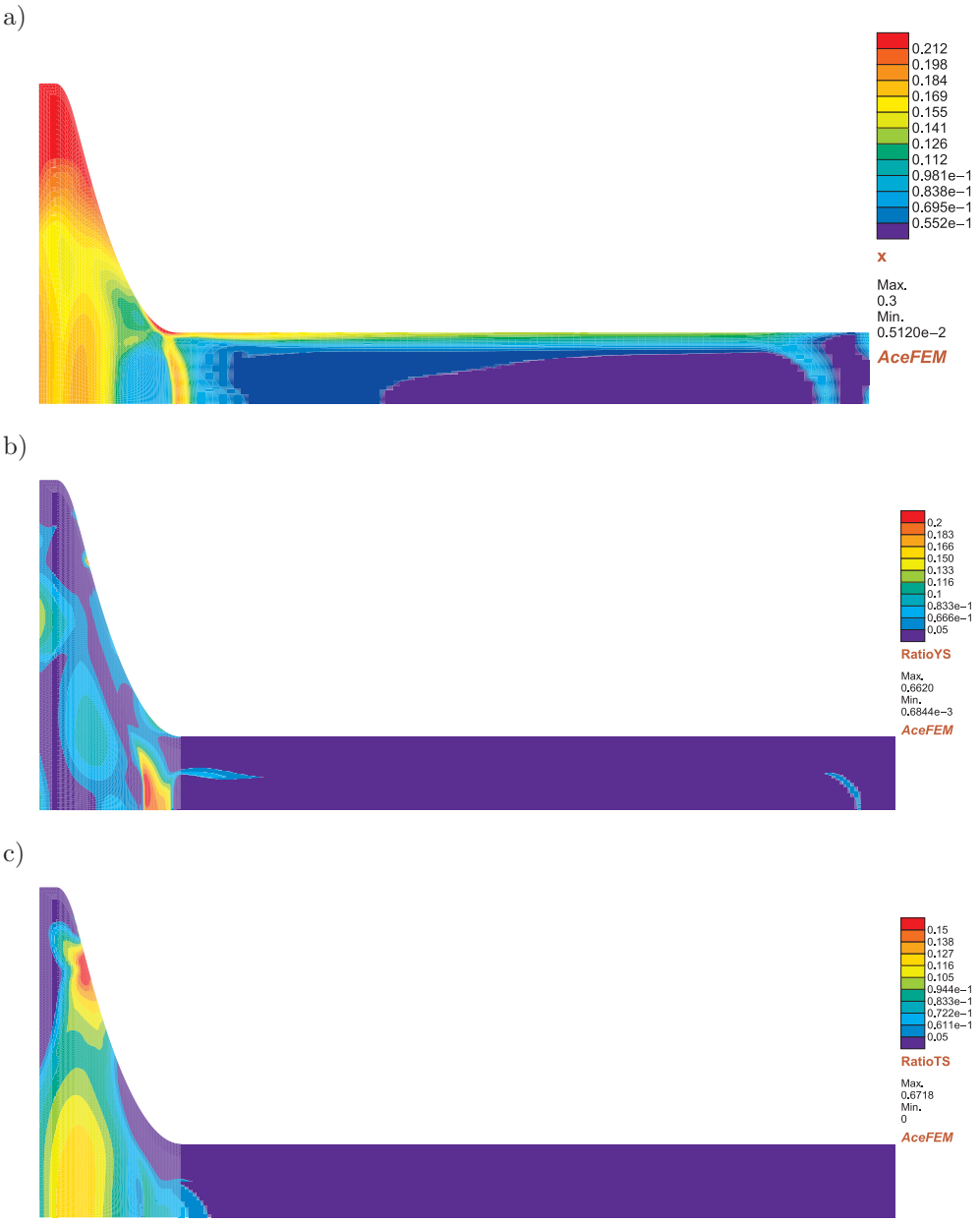

Fig. 7. Ceramic exhaust valve analysis with optimal (for $\beta = 1.0$ in Eq. (17)), inhomogeneous distribution of ceramic phase. Distribution of: a) volume fraction of ceramic phase x, b) measure of effective stresses J_{pl}, c) measure of tensile stresses J_{cr}. The maximum value of J_{pl} was reduced in comparison to its value at the beginning of optimization process while the maximum value of J_{cr} was increased, see Fig. 3.

The evolutions of J_{cr} and J_{pl} for final ceramic distribution are presented in Fig. 6. The comparison of the highest values from Fig. 4 and Fig. 6 allows us to conclude that the process of phase optimization significantly reduced the maximum values of J_{pl}, while increases the maximum values of J_{cr}. This is the type of a trade-off design, typical for thermomechanical problems.

Several simulations with different form of the objective functional have been performed. The parameter β in Eq. (17) was assumed to be equal one, two, and three. Additionally, the optimization procedures started from homogeneous density of ceramic phase equal to $x_{ini} = 0.0$ or $x_{ini} = 0.3$. Paths of optimization processes are plotted in Fig. 8. The different optimization functionals (corresponding to different values of the weight factor β) lead to different optimal distributions of the ceramic phases.

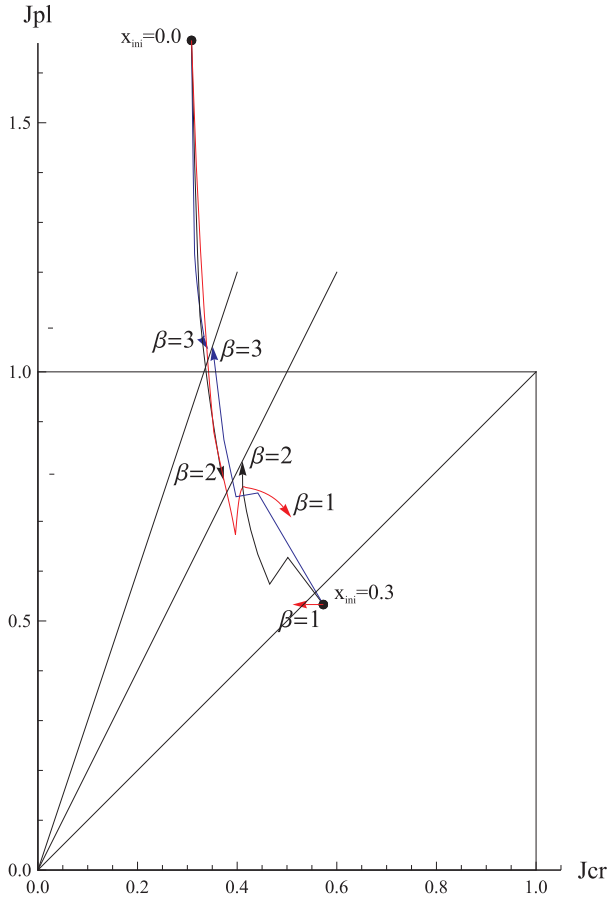

Fig. 8. Paths of optimization processes with the parameter β in Eq. (17) equals one (denoted with red arrows), two (black arrows), and three (blue arrows). Optimization procedures start from the state of homogeneous density of ceramic phase equal to $x_{ini} = 0.0$ or $x_{ini} = 0.3$.

7. Summary and conclusions

The robust optimization method of FGM under combined cyclic thermal and mechanical loading is proposed. The methodology is especially useful in the design procedure of elements with complex shapes and under complex transient loading conditions.

The presented numerical example illustrates the optimal volume fraction distribution of the ceramic phase Al_2O_3 within the metal matrix of NiAl for mechanical and thermal constraints. The analysis of FGM engine valves was significantly simplified allowing optimization of lightweight valves. Our method permits manufacturing of products with improved surface properties (low-wear surface) and with reduced weight. It is worth to note that valves with standard ceramic coating are subjected to very high thermal stresses caused by the difference between thermal expansion coefficients of ceramic coating and bulk material. The current manufacturing technologies allow for producing reinforced metal matrix NiAl with ceramic phase of Al_2O_3. Thus, the proposed method seems very useful for practical design of thermal resistant structures made of graded materials.

The objective functional used represents the sensitivity of structure on incidentally applied high stresses, see Eqs. (17), (30), (31), (35), (36). Other measures, like the integrated measures over time period of engine operation $J^t_{cr} = \int J_{cr}\, dt$ and $J^t_{pl} = \int J_{pl}\, dt$, proposed by Eq. (16), provide the global assessment of safety of valve relative to fatigue failure. Such modifications allow for flexible adjustment of the objective functional to the particular need. Additionally, the method permits avoiding *a priori* specification of an FGM variation function. The extended numerical analysis with account for global and local objective functions and their sensitivity derivatives will be presented in the subsequent paper.

An alternative approach based on thermo-elastic-plastic stress analysis under cyclic loading conditions and requirement of an elastic shake-down in the steady state could also provide the distribution of ceramic phase. However, the attainment of shake-down state does not assure the control of cracking and damage growth. Therefore the present approach, based on thermoelastic analysis, seems much simpler and reliable.

Acknowledgements

This work was supported by the EU FP7 Project "Micro and Nanocrystalline Functionally Graded Materials for Transport Applications" (MATRANS) under Grant Agreement no. 228869 and by State Committee for Scientific Research in Poland under Grant no. N501 092135.

References

[1] M.P. Bendsøe. *Optimization of Structural Topology, Shape, and Material*. Springer, 1995.
[2] V. Birman, L.W. Byrd. Modeling and analysis of functionally graded materials and structures. *Applied Mechanics Reviews*, **60**(5): 195–216, 2007.
[3] D. Boussaa. Optimizing the composition profile of a functionally graded interlayer using a direct transcription method. *Computational Mechanics*, **39**(1): 59–71, 2006.
[4] M. Burger, B. Hackl, W. Ring. Incorporating topological derivatives into level set methods. *Journal of Computational Physics*, **194**(1): 344–362, 2004.
[5] N. Chawla, Y.-L. Shen. Mechanical behavior of particle reinforced metal matrix composites. *Advanced Engineering Materials*, **3**(6): 357–370, 2001.
[6] J.R. Cho, D.Y. Ha. Volume fraction optimization for minimizing thermal stress in Ni-Al_2O_3 functionally graded materials. *Materials Science and Engineering: A*, **334**(1–2): 147–155, 2002.
[7] K. Dems, Z. Mróz. Variational approach to sensitivity analysis in thermoelasticity. *Journal of Thermal Stresses*, **10**(4): 283–306, 1987.
[8] K. Dems, Z. Mróz. Methods of sensitivity analysis. In M. Kleiber, editor, *Handbook of Computational Solid Mechanics: Survey and Comparison of Contemporary Methods*, pages 673–755. Springer-Verlag, Berlin, 1998.
[9] K. Dems, Z. Mróz. Sensitivity analysis and optimal design of external boundaries and interfaces for heat conduction systems. *Journal of Thermal Stresses*, **21**(3–4): 461–488, 1998.
[10] H.A. Eschenauer, N. Olhoff. Topology optimization of continuum structures: A review. *Applied Mechanics Reviews*, **54**(4): 331–390, 2001.
[11] Z. Hashin, S. Shtrikman. A variational approach to the theory of the elastic behaviour of multiphase materials. *Journal of the Mechanics and Physics of Solids*, **11**(2): 127–140, 1963.
[12] J. Korelc. Multi-language and multi-environment generation of nonlinear finite element codes. *Engineering with Computers*, **18**(4): 312–327, 2002.
[13] Z. Mróz. Variational methods in sensitivity analysis and optimal design. *Journal of Mechanics A/Solids*, **13**(2): 115–147, 1994.
[14] K.-S Na, J.-H Kim. Volume fraction optimization of functionally graded composite panels for stress reduction and critical temperature. *Finite Elements in Analysis and Design*, **45**(11): 845–851, 2009.
[15] S.J. Osher, R. Fedkiw. *Level set methods and dynamic implicit surfaces*. Springer, New York, 2003.
[16] J.H. Rong, Q.Q. Liang. A level set method for topology optimization of continuum structures with bounded design domains. *Computer Methods in Applied Mechanics and Engineering*, **197**(17–18): 1447–1465, 2008.
[17] J.A. Sethian. *Level set methods and fast marching methods: evolving interfaces in computational geometry, fluid mechanics*. Cambridge University Press, 1999.
[18] M.H. Shojaefard, A.R. Noorpoor, D.A. Bozchaloe, M. Ghaffarpour. Transient thermal analysis of engine exhaust valve. *Numerical Heat Transfer, Part A: Applications*, **48**(7): 627–644, 2005.
[19] W. Szymczyk. Numerical simulation of composite surface coating as a functionally graded material. *Materials Science and Engineering: A*, **412**(1–2): 61–65, 2005.
[20] S. Turteltaub. Functionally graded materials for prescribed field evolution. *Computer Methods in Applied Mechanics and Engineering*, **191**(21–22): 2283–2296, 2002.
[21] M. Yulin, W. Xiaoming. A level set method for structural topology optimization and its applications. *Advances in Engineering Software*, **35**(7): 415–441, 2004.
[22] U. Zrahia, P.B. Yoseph. Alternative designs towards thermal optimization of coated valves using space-time finite elements. *International Journal of Numerical Methods for Heat & Fluid Flow*, **5**(3): 189–206, 1994.